Supporting Information

P-block metal atoms induced the spin state transition of Fe-N-C catalyst for efficient oxygen reduction

Jiana Chen[#], Tingyi Zhou[#], Changjie He, Zhaoyan Luo*, Chuan Shi, Lei Zhang, Qianling Zhang, Chuanxin He, Xiangzhong Ren*

College of Chemistry and Environmental Engineering, Shenzhen University, Shenzhen, Guangdong 518060, P.R. China.

Corresponding author:

Xiangzhong Ren, Email: renxz@szu.edu.cn

Zhaoyan Luo, Emai: luozhaoyan@szu.edu.cn

#These authors contributed equally to this work

1. Experimental section

1.1. Materials

Chemicals. $Zn(NO_3)_2 \cdot 6H_2O$, 2-methylimidazole, $Fe(acac)_3$, SnO_2, $SbCl_3$, Dicyanodiamide, $Bi(NO_3)_3 \cdot H_2O$, Ethylene glycol, methanol and polyvinyl alcohol (PVA) were obtained from Aladdin Company. High-purity $HClO_4$ and 5 wt% Nafion ionomer were purchased from Sigma. Commercial state-of-the-art 20 wt% Pt/C (Johnson Matthey Company, HiSPEC™ 3000) was used as the benchmark for comparison. Other chemicals were provided by Beijing Chemical Works. Ultrapure water was used throughout all experiments.

1.2. Synthesis of Fe, M-N-C (M=Sn, Sb, Bi)

Fe@ZIF-8: Initially, 2-methylimidazole (6.5 g 80 mmol), $Fe(acac)_3$ (0.88 g 2.5 mmol), $Zn(NO_3)_2 \cdot 6H_2O$ (3.0 g 10 mmol) were added to 120 mL of methanol and stirred for 12 hours. Following this, the solution was washed three times by centrifugation with ethanol, and then dried overnight to obtain Fe@ZIF-8.

Fe, Sn-N-C: Fe@ZIF-8 was heated at a rate of 5 °C min^{-1} to 950 °C for 1 hour in a N_2 atmosphere. After cooling, the product was ground to obtain Fe-N-C. The introduction of Sn element was carried out by chemical vapor deposition (CVD). A porcelain boat containing 1.0g of SnO_2 was placed in front of a boat containing 0.4g of Fe-N-C powder. The samples were heated at a rate of 5 °C min^{-1} to 250 ℃ for 1 hour in an Ar atmosphere, then heated to 750 ℃ for 1 hour, and further heated at a rate of 2 °C min^{-1} to 950 °C for 1 hour, After cooling to room temperature, etching was performed with a 0.1M HCl solution for 12 hours. The resulting product was washed with deionized water and filtered and dried to obtain Fe, Sn-C-N.

Fe, Sb-N-C: $SbCl_3$ (57 mg) was added to 50 ml of ethanol. Under sonication, 500 mg of prepared Fe@ZIF-8 and 841 mg of dicyandiamide were added to the mixture. Sonication was carried out at room temperature for 2 hours, followed by stirring for 4 hours. The mixture was washed three times by centrifugation with ethanol, then centrifuged and separated, and finally dried at 60 °C for 12 hours to obtain Fe, Sb-ZIF-8. The Fe, Sb-ZIF-8 was heated at a rate of 5 °C min^{-1} to 950 ℃ for 2 hours in an Ar atmosphere. After cooling, the carbide powder was collected, followed by etching with 0.1M HCl solution for 12 hours, the resulting product was washed by

deionized water, filtered and dried to obtain Fe, Sb-N-C.

Fe, Bi-N-C: Following a procedure similar to that of Fe, Sb-N-C , dissolve 48 mg of $Bi(NO_3)_3 \cdot H_2O$ in 50 ml of ethylene glycol instead of dissolving $SbCl_3$ in 50 ml of ethanol. The resulting mixture is referred to as Fe, Bi-ZIF-8 before carbonization.

M-N-C (M=Sn, Sb, Bi): Following a procedure similar to that of Fe,Sb-N-C, but without adding $Fe(acac)_3$ during the synthesis process. The sample before carbonization is named M-ZIF-8(M=Sn, Sb, Bi).

Fe-N-C: Following a procedure similar to that of Fe,Sb-N-C, but without adding $SbCl_3$ during the synthesis process. The sample before carbonization is named Fe-ZIF-8.

N-C: Following a procedure similar to that of Fe,Sb-N-C procedure, but without adding $SbCl_3$, $Fe(acac)_3$, Zn $(NO_3)_2 \cdot 6H_2O$ during the synthesis process. The sample before carbonization is named ZIF-8.

1.3. Physical Characterization

X-ray powder diffractometry (XRD, Empyrean, Cu Kα radiation) was utilized to characterize the crystalline phases of the samples. Field emission scanning electron microscopy with energy spectrometry (FESEM, JSM-7800F & TEAM Octane Plus) and transmission electron microscopy (TEM, JEM-2100 & X-Max80) were employed to observe the microscopic morphology of the samples. X-ray photoelectron spectroscopy (XPS, K-Alpha+) was employed to obtain the valence distribution of the elements in the samples. Raman spectroscopy (inVia) spectra were obtained to analyze the carbon structure of the samples. The elemental content was measured using inductively coupled plasma mass spectrometer (ICP-MS). The Fe K-edge XAFS was tested at the BL14W1 station of the Shanghai Synchrotron Radiation Facility (SSRF).

1.4. Calculation of the number of unpaired electrons in the metal site:

The effective magnetic moments (μ_{eff}) can be obtained by fitting the susceptibility (χ):

$$\chi = M/H \tag{1}$$

Here, χ obeys the Curie–Weiss law:

$$\chi = C/(T - \Theta) \tag{2}$$

where Θ is the Curie–Weiss temperature, T is the temperature, and C is the Curie constant. C

could be evaluated from the χ^{-1}–T curves shown in Figure 3a. The μ_{eff} could be obtained using the following equation according to the Langevin theory:

$$\mu_{eff} = \sqrt{8}C\mu_B \quad (3)$$

where μ_B is the Bohr magneton.

Here, μ_{eff} can be expressed as follows:

$$\mu_{eff} = g\sqrt{S(S+1)}\mu_B = \sqrt{n(n+2)}\mu_B \quad (4)$$

where g is the Lande factor (g=2), S is the total spin quantum number, and n is the number of unpaired electrons. The μeff and n of FeN_4 and RuN_4 could be determined from Eqs. (3) and (4).

The μeff of FeN_4/RuN_4 includes contributions from both Ru and Fe, meaning that the μeff obeys Eq. (5):

$$\mu_{eff}^2 = \mu_{eff,1}^2 + \mu_{eff,2}^2 \quad (5)$$

where $\mu eff,1$ and $\mu eff,2$ are the magnetic moments of Ru and Fe, respectively.

The total effective magnetic moments μ_{eff}, total could be calculated using Eqs. (6) and (7):

$$\mu_{eff,total} = g\sqrt{S_1(S_1+1)V_1 + S_2(S_2+1)V_2}\mu_B = \sqrt{n_1(n_1+2)V_1 + n_2(n_2+2)V_2}\mu_B \quad (6)$$

$$V_1 + V_2 = 1 \quad (7)$$

where $S1$ and $S2$ are the total spin quantum numbers of Ru and Fe, n1 and n2 are the numbers of unpaired electrons of Ru and Fe, and V1 and V2 are the molar percentages of Ru and Fe, respectively.

1.5. Electrochemical characterizations

The electrochemical performance was evaluated using the 750E Bipotentiostat (CH Instruments). Non-platinum catalyst ink was prepared by ultrasonically dispersing 5 mg of catalyst in a suspension containing 50 μL Nafion (5 wt%) solution and 950 μL ethanol. In contrast, 20 wt% Pt/C catalyst ink was prepared by dispersing 5 mg catalyst ultrasonically in a mixture solution containing 50 μl Nafion (5 wt%) solution, 550 μL of isopropanol and 400 μL of Milli-Q water. The catalyst film-coated electrode was obtained by dispersing the catalyst ink on a glassy carbon rotating disk electrode or rotating ring-disk electrode, followed by drying in air. The catalyst

loadings on RDE or RRDE were 0.8 mg cm^{-2} for non-noble metal catalyst and 40 μg_{pt} cm^{-2} for Pt/C catalyst. All potentials are provided vs. RHE.

A 0.1 M $HClO_4$ (or 0.1 M KOH) solution served as the electrolyte for ORR test. A conventional three-electrode cell was utilized, incorporating a saturated calomel electrode (SCE) (or Ag/AgCl electrode) as the reference electrode, a graphite rod as the counter electrode, and the catalyst film coated RDE or RRDE as the working electrode. RDE or RRDE measurements were conducted by linear sweep voltammetry (LSV) from 1.1 V to 0.1 V at a scan rate of 5 mV s^{-1} at 1600 rpm, while the ring electrode was held at 1.3 V versus. RHE.

The H_2O_2 collection coefficient at the ring in RRDE experiments was measured to be 0.37, using a $Fe(CN)_6^{4-/3-}$ redox couple. The following equations were employed to calculate n (the apparent number of electrons transferred during ORR) and % H_2O_2 (the percentage of H_2O_2 released during ORR)

$$n = \frac{4I_D}{I_D + (I_R/N)}$$

$$\%H_2O_2 = 100\frac{2I_R/N}{I_D + (I_R/N)}$$

where I_D represents the faradaic at the disk, I_R is the faradaic current at the ring, and N is the H_2O- collection coefficient at the ring.

Accelerated durability tests (ADTs) were performed at room temperature in O_2-saturated 0.1 M $HClO_4$ (or 0.1 M KOH) solution by applying cyclic potential sweeps between 0.6 and 1.0 V versus RHE at a sweep rate of 200 mV s^{-1} for 10000 cycles and collect thecv initial and final LSV curves.

1.6 Zn-air Batteries test

For the Zn-air battery test, the air electrode was prepared by uniformly coating the as-prepared catalyst ink onto carbon paper then drying it at 80°C for 4 h. The catalyst loading was 1mg cm^{-2}. A Zn plate was used as the anode. Both electrodes were assembled into a Zn-air battery, and 6 M KOH aqueous solution with 0.2 M $Zn(CH_3COO)_2$ was used as the electrolyte. The Galvano dynamic charge and discharge profiles of the battery were obtained by scaling the current density from 0 to 250 mA cm^{-2}. The cycling tests were conducted at a current density of 5 mA cm^{-2} with 15 min discharge and 15 min charge time for each cycle. The tests were operated in ambient air

condition.

Assembly of flexible solid-state Zn-Air battery.

The catalyst films, waterproof, breathable membrane, and the current collector are sequentially stacked to form an air cathode. The anode is a polished zinc foil (0.3 mm), and the solid electrolyte is 6 M KOH + 0.2 M $Zn(OAc)_2$ filled PAM/MMT organic hydrogel. The catalyst films were prepared by dispersing 30 mg of catalyst and 5 mg of acetylene carbon in ethanol and stirring for 10 min. Then 5 ml of polytetrafluoroethylene (PTFE) emulsion was dropped in and stirred for 5 min, and then rolled into a catalyst film with a thick of 0.2 mm. To prepare the gel polymer electrolyte, firstly, 5 g acrylamide (AM), 5 mg N-N methylene bisacrylamide (MBA), and 12.5 mg

potassium persulfate (KPS) was added into 20 ml mixed solvent of deionized water and dimethyl sulfoxide (DMSO) (deionized water: DMSO = 1:1). The obtained solution was stirred at room temperature for 0.5 h. Then 15 mg MMT was added and the obtained mixture was kept stirring for another 0.5 h, then was moved to the mold. Polymerization occurred at 60°C for 12 h. After cooling, the obtained PAM/MMT organic hydrogel was immersed in 6 M KOH + 0.2 M $Zn(OAc)_2$ solution for 72 h. Lastly, the air electrode and zinc foil were placed on the two sides of the PAM/MMT gel respectively to form a flexible Zn-air battery.

Test of battery performance.

Polarization curves were measured by LSV (5 mV s^{-1}) on CHI630e electrochemical workstation. Current density and power density were standardized with the effective surface area of the air electrode. The specific capacity is calculated according to the following equation:

$$specific\ capacity = \frac{current * service\ hours}{weight\ of\ consumed\ zinc}$$

The energy density is calculated according to the following equation:

$$energy\ density = \frac{current * service\ hours * average\ discharge\ voltage}{weight\ of\ consumed\ zinc}$$

The galvanostatic discharge-charge test was performed on a NEWARE CT4008T multi-channel battery testing system. Cycles were conducted by the electrochemical pulse method at a constant current density of 5 mA cm^{-2}. Each cycle consisted of 10 minutes of discharge followed by 10

minutes of charge.

Supplementary figures

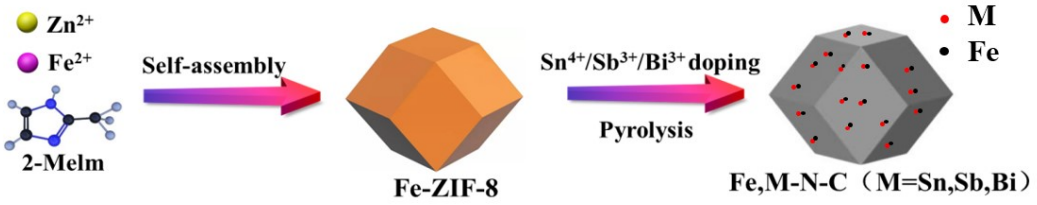

Figure S1. Synthetic routes of Fe,M-N-C(M=Sn, Sb, Bi)

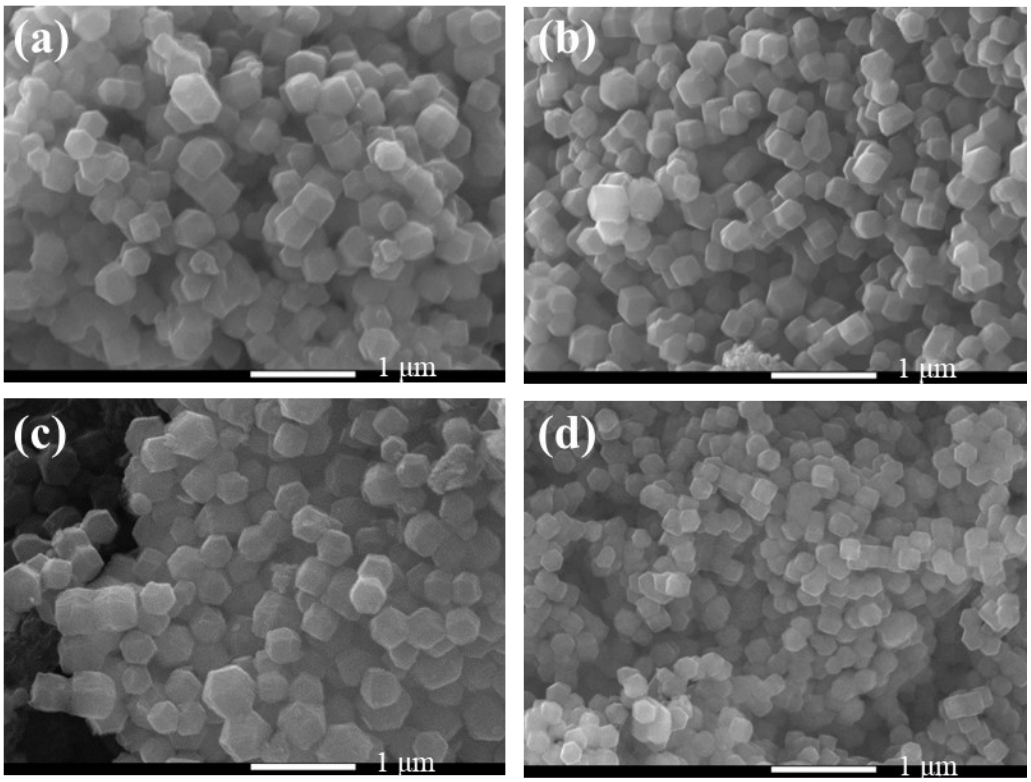

Figure S2. (a) SEM of Fe,Sn-N-C catalyst; (b) SEM of Fe,Sb-N-C catalyst; (c) SEM of Fe,Bi-N-C catalyst; (d) SEM of Fe-N-C catalyst.

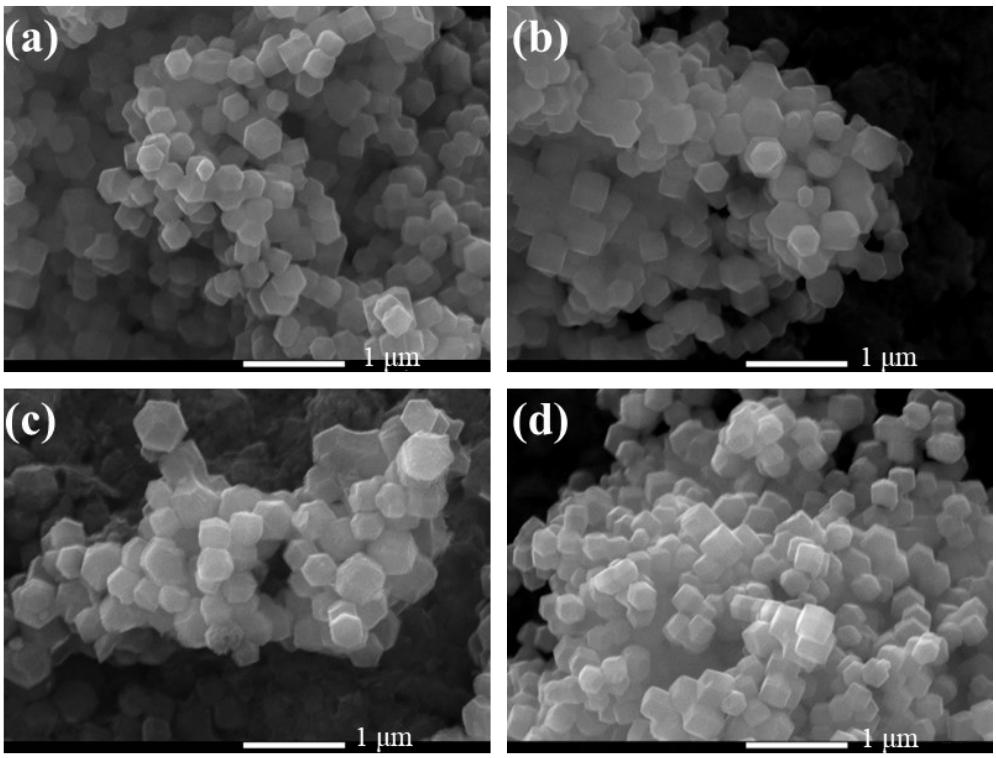

Figure S3. (a) SEM of Sn-N-C catalyst; (b) SEM of Sb-N-C catalyst; (c) SEM of Bi-N-C catalyst; (d) SEM of N-C catalyst.

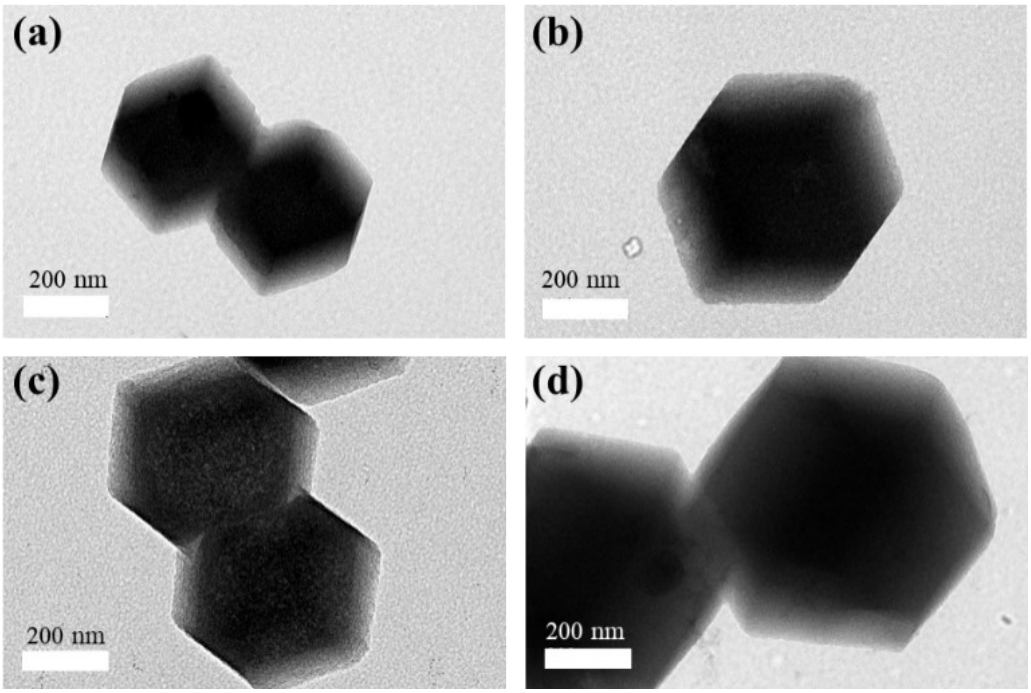

Figure S4. (a)TEM of Fe,Sn-N-C catalyst; (b)TEM of Fe,Sb-N-C catalyst; (c)TEM of Fe,Bi-N-C catalyst; (d)TEM of Fe-N-C catalyst.

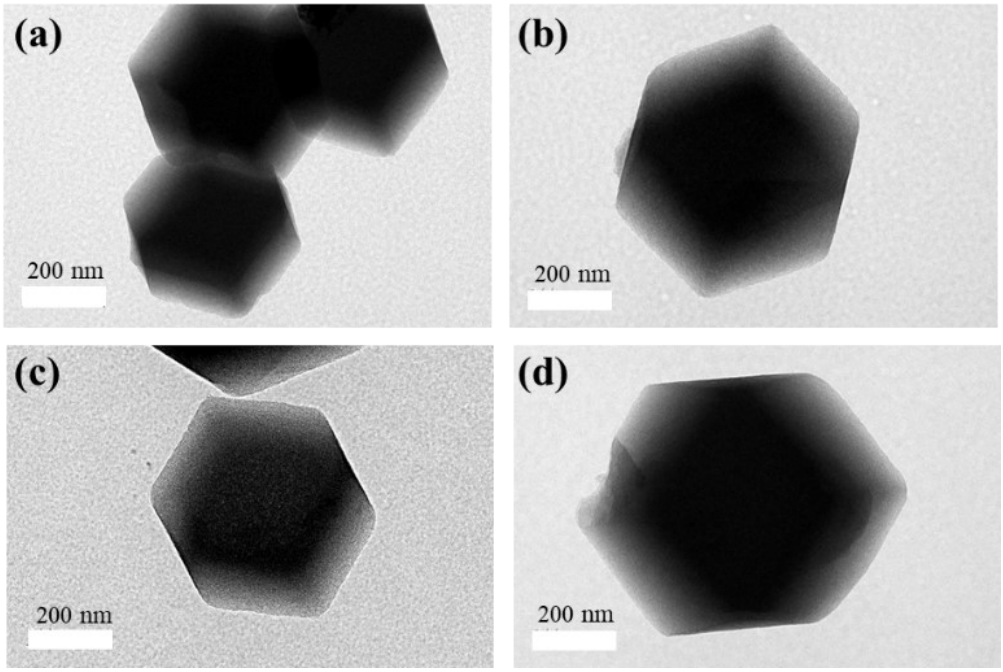

Figure S5. (a)TEM of Sn-N-C catalyst; (b)TEM of Sb-N-C catalyst; (c)TEM of Bi-N-C catalyst. (d)TEM of N-C catalyst.

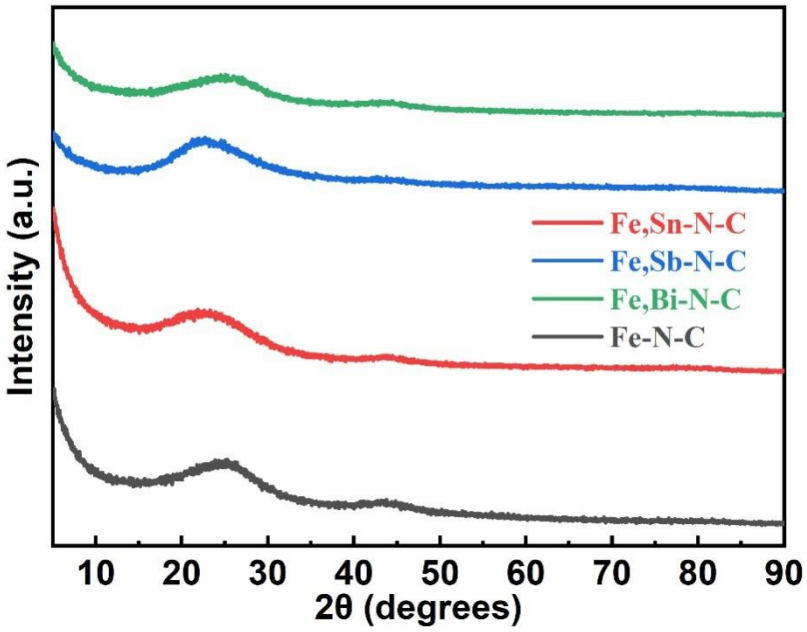

Figure S6. XRD patterns of Fe,Sn-N-C, Fe,Sb-N-C, Fe,Bi-N-C, Fe-N-C.

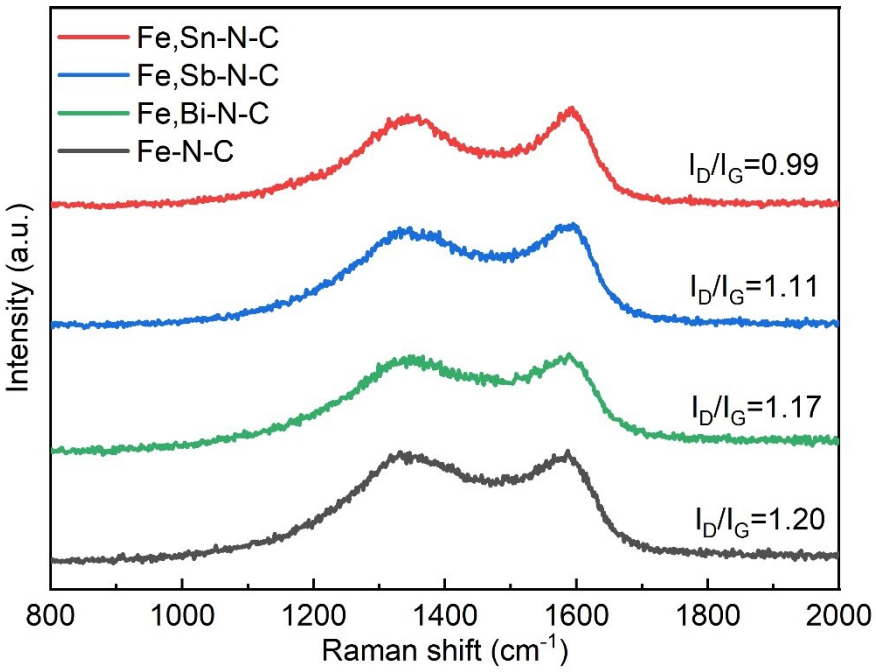

Figure S7. Raman patterns of Fe,Sn-N-C, Fe,Sb-N-C, Fe,Bi-N-C, Fe-N-C.

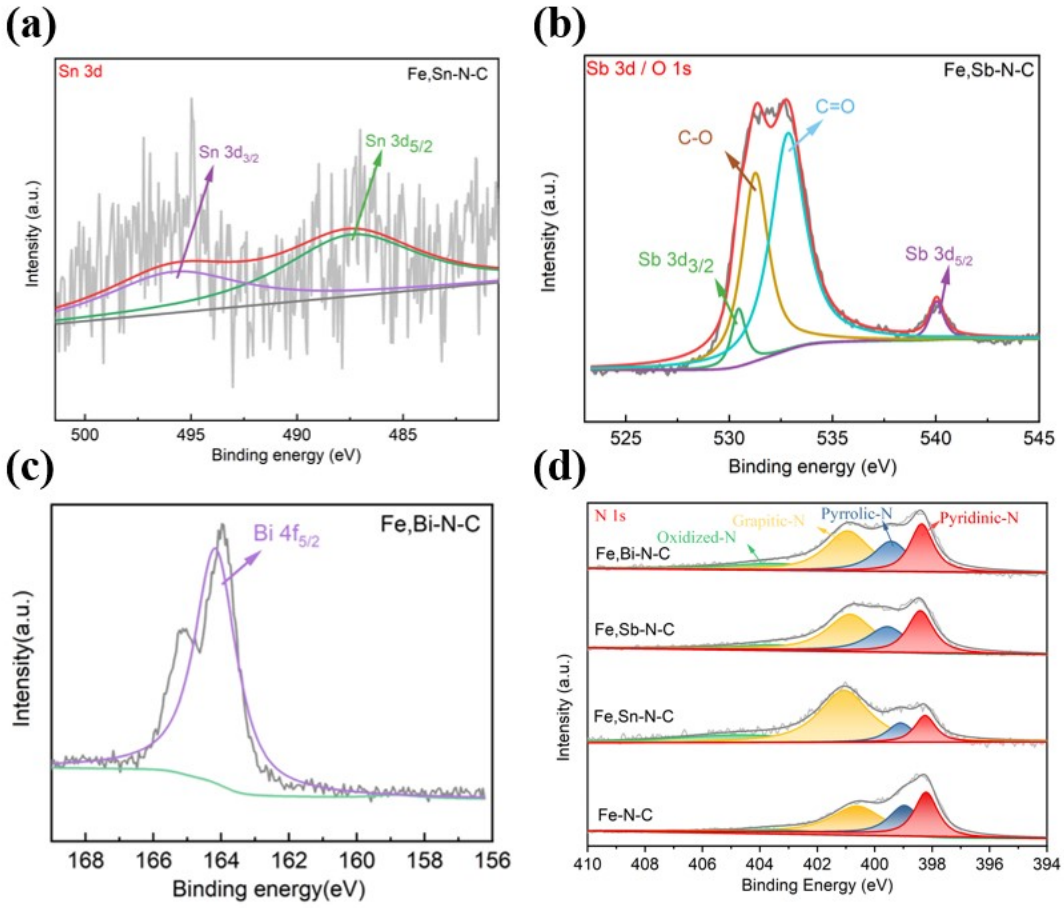

Figure S8. (a) Sn 3d XPS Spectra of Fe,Sn-N-C catalyst; (b) Sb 3d/ O 1s XPS Spectra of Fe,Sb-N-C catalyst; (c) Bi 4f XPS Spectra of Fe,Bi-N-C catalyst; (d) N 1s XPS Spectra of Fe,M-N-C(Sn, Sb, Bi) and Fe-N-C

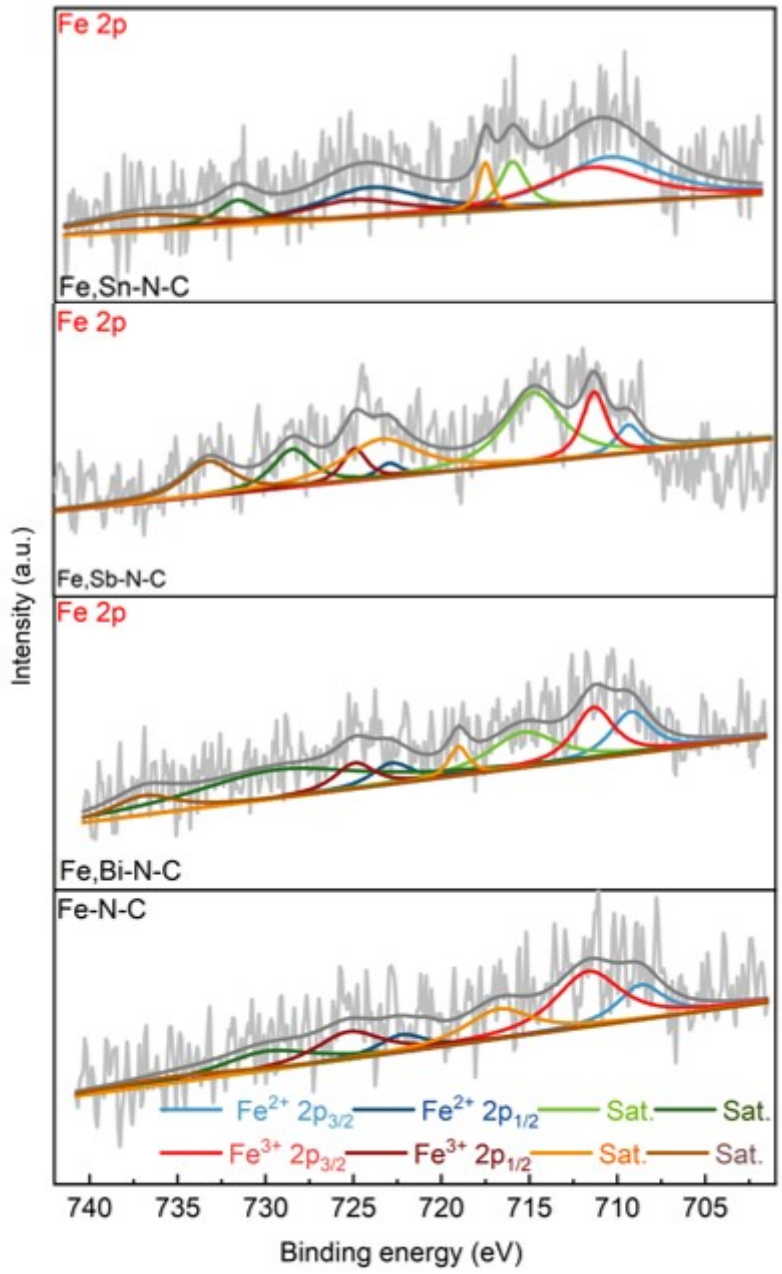

Figure S9. Fe 2p XPS Spectra of Fe,M-N-C (M=Sn, Sb, Bi)and Fe-N-C.

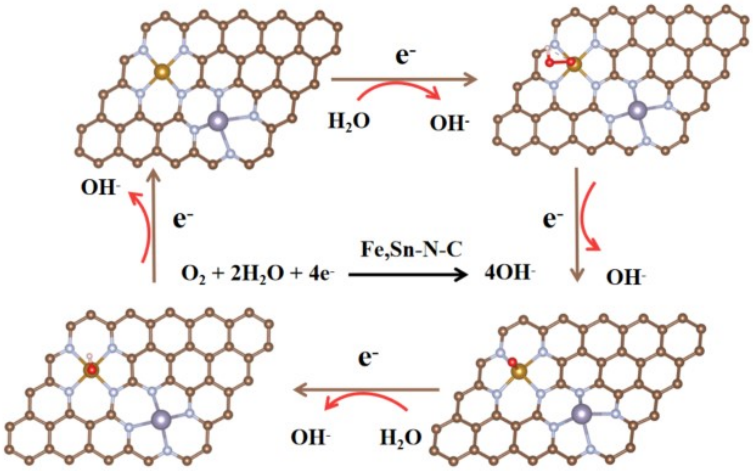

Figure S10. ORR diagram using Fe,Sn-N-C as catalyst.

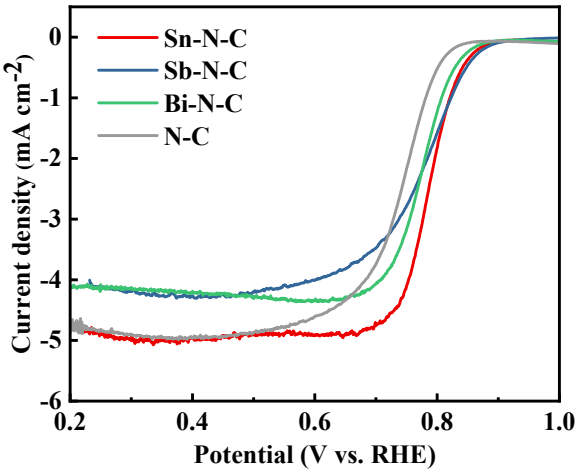

Figure S11. ORR polarization curves of Sn-N-C, Sb-N-C, Bi-N-C and N-C catalysts recorded in the 0.1 M KOH.

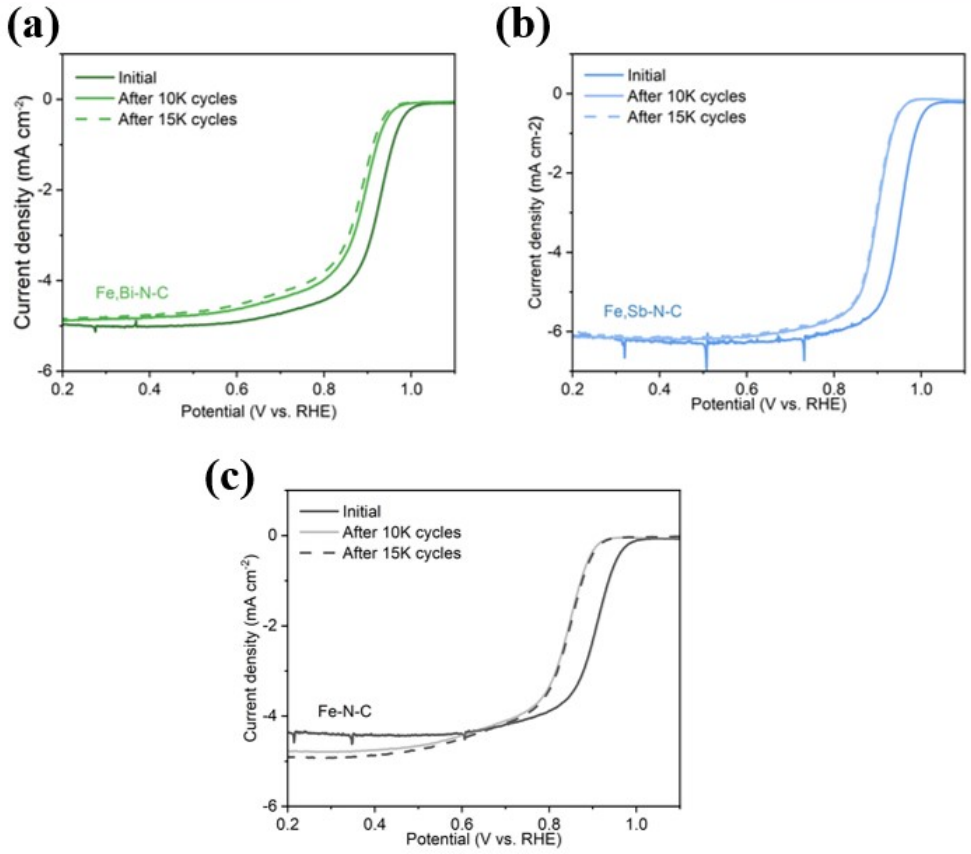

Figure S12. ORR polarization curves of (a) Fe,Bi-N-C (b) Fe,Sb-N-C and (c) Fe-N-C catalysts recorded in the 0.1 M KOH before and after ADT.

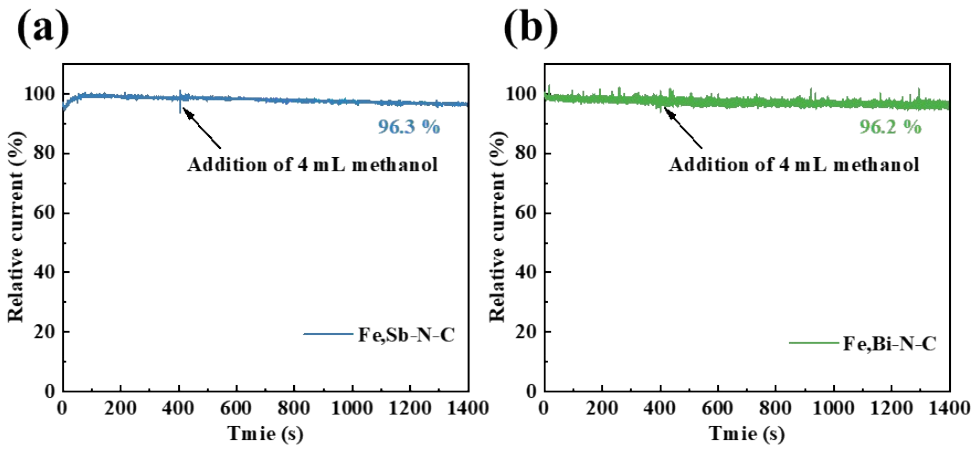

Figure S13.Chronoamperometric responses of Fe,Sb-N-C (a) and Fe,Bi-N-C (b) in O_2 saturated 0.1 M KOH with 4 mL methanol injected at 400 s. Rotation speed: 1600 rpm.

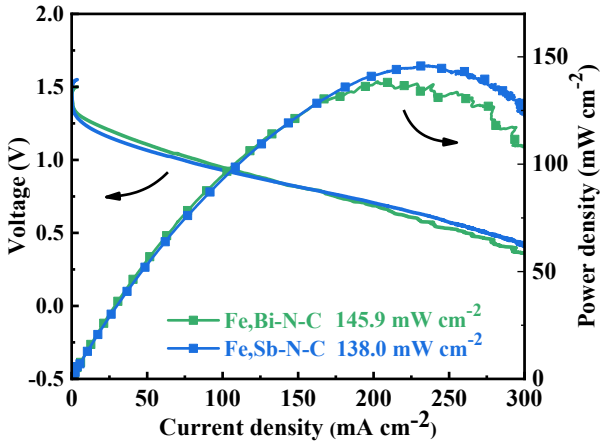

Figure S14. Discharge polarization curves and the corresponding power density curves of Zn-air batteries assembled with Fe,Sb-N-C and Fe,Bi-N-C.

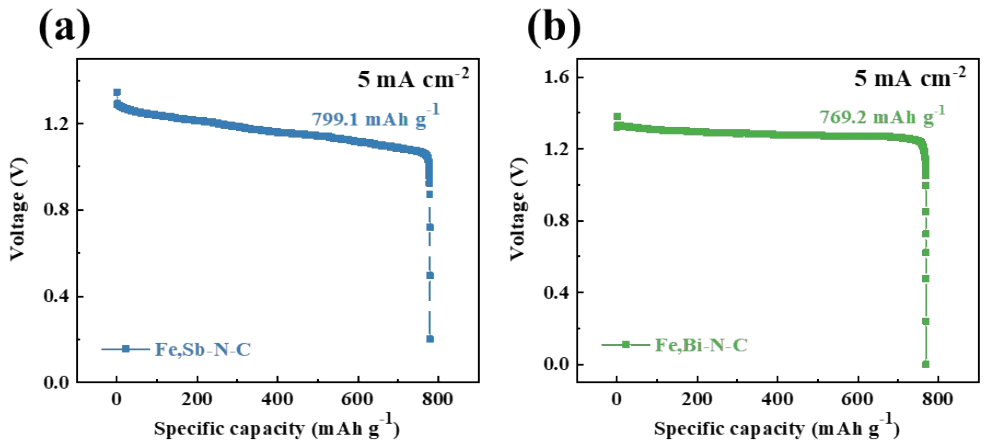

Figure S15. Specific capacity of Zn–air battery at 5 mA cm^{-2} of Zn-air batteries assembled with Fe,Sb-N-C (a) and Fe,Bi-N-C (b).

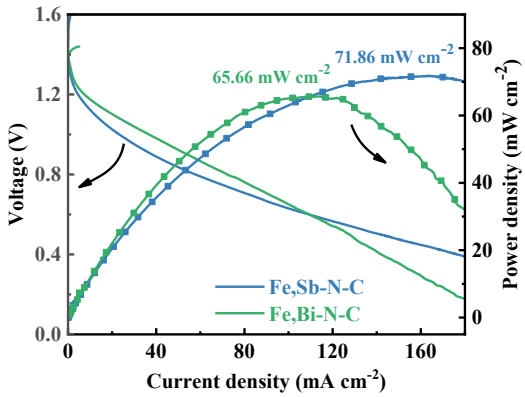

Figure S16. Discharge polarization curves and the corresponding power density curves of solid-state Zn-air battery assembled with Fe,Sb-N-C and Fe,Bi-N-C.

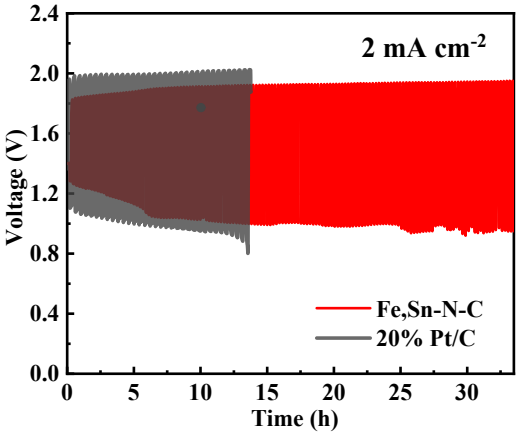

Figure S17. Cycling tests at the current density of 2 mA cm^{-2} of Fe,Sn-N-C solid battery and Pt/C-based solid battery.

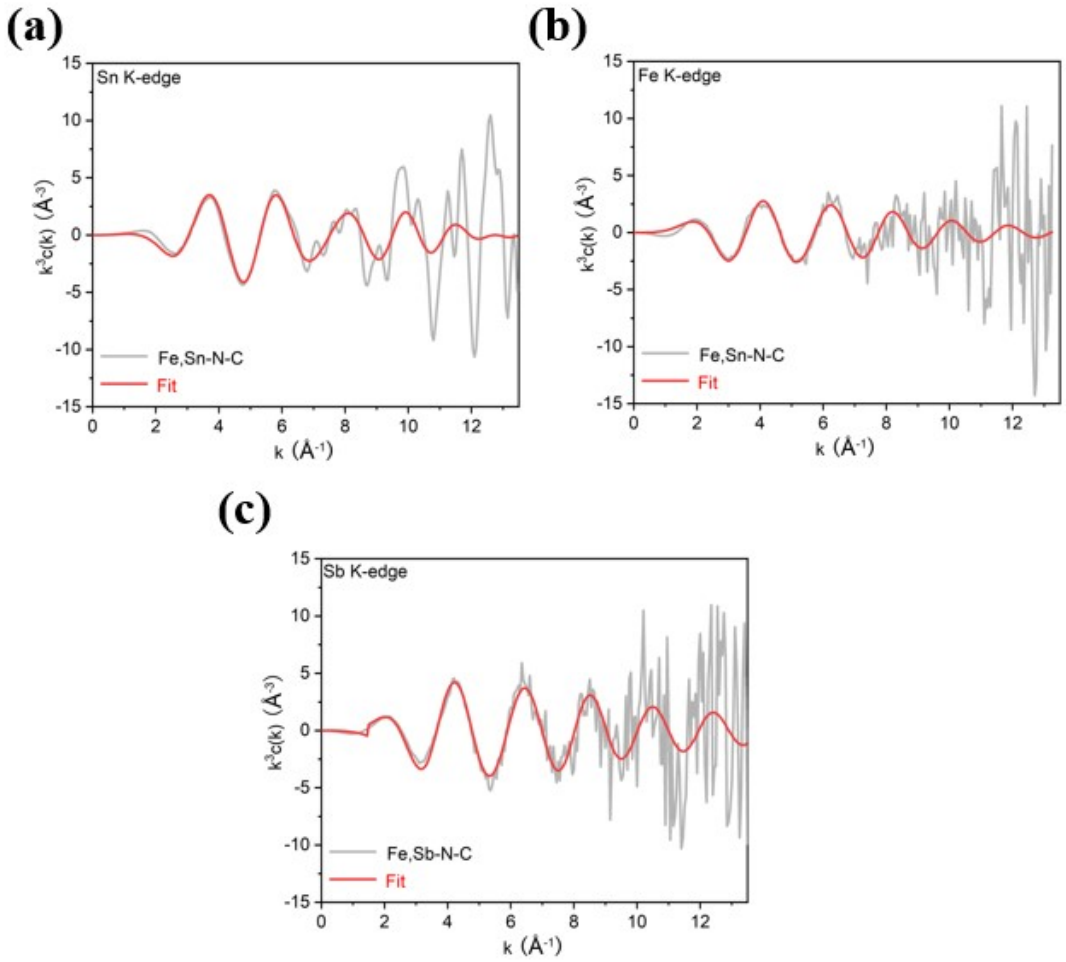

Figure S18. (a) Sn K-edge EXAFS fitting curves of Fe,Sn-N-C; (b) Fe K-edge EXAFS fitting curves of Fe,Sn-N-C; (c) Sb K-edge EXAFS fitting curves of Fe,Sb-N-C.

Table S1. The metal loading of Fe,M-N-C and Fe-N-C measured by ICP-MS

Catalyst	Fe(wt%)	Sn (wt%)	Sb (wt%)	Bi (wt%)
Fe,Sn-N-C	0.56	0.50	-	-
Fe,Sb-N-C	0.63	-	1.38	-
Fe,Bi-N-C	0.27	-	-	0.47
Fe-N-C	0.35	-	-	-

Table S2. EXAFS fitting parameters at the Fe K-edge various samples（S_0^2=0.72）

Sample	Path	C.N.	R （Å）	$\sigma^2\times10^3$ （Å^2）	ΔE （eV）	R factor
Fe foil	Fe-Fe	8*	2.46±0.01	2.1±0.9	4.3±1.0	0.001
	Fe-Fe	6*	2.84±0.01	2.0±1.3	3.0±2.0	
Fe Sample	Fe-N	4*	2.03±0.02	7.5±3.1	0.1±2.2	0.019

Table S3. EXAFS fitting parameters at the Sn K-edge various samples（S_0^2=0.88）

Sample	Path	C.N.	R （Å）	$\sigma^2\times10^3$ （Å^2）	ΔE （eV）	R factor
Sn foil	Sn-Sn	6*	3.00±0.01	10.5±0.7	3.5±0.8	0.017
Sn Sample	Sn-N	4*	2.07±0.01	8.9±2.5	-5.9±1.7	0.005
	Sn-O	1*	2.66±0.02	3.7±4.8		

Table S4. EXAFS fitting parameters at the Sb K-edge various samples（S_0^2=0.82）

Sample	Path	C.N.	R (Å)	$\sigma^2\times10^3$ ($Å^2$)	ΔE (eV)	R factor
Sb foil	Sb-Sb	6*	2.09±0.01	5.0±0.4	6.4±0.8	0.015
Sb sample	Sb-N	4*	1.97±0.01	3.3±4.6	8.3±3.0	0.016
	Sb-O	1*	2.07±0.11			